

Thermal-lens measurement in a side-pumped 1.3- μm Nd:YVO₄ bounce laser

Masahito Okida^a, Akihiro Tonouchi^b, Masahide Itoh^a,
Toyohiko Yatagai^a and Takashige Omatsu^{b,c}

^a*Institute of Applied Physics, University of Tsukuba, 1-1-1, Tennodai, Tsukuba,
Ibaraki, 305-8573, Japan*

^b*Department of Information and Image Science, Chiba University, 1-33 Yayoi-cho,
Inage-ku, Chiba, 263-8522, Japan*

^c*Japan Science and Technology Agency, 4-1-8, Honcho, Kawaguchi, Saitama,
Japan*

Abstract: We investigated thermal-lensing effects in a side-pumped 1.3- μm Nd:YVO₄ slab laser amplifier having a bounce geometry. The thermal-lens power during 1.3 μm laser action was 1.3-times larger than that without laser action. Excited-state absorption is the main cause for increased heat loading during laser operation. The heat-loading formula in end-pumped 1.3- μm vanadate lasers having low Nd doping can be extended to account for heat generation in diode-side-pumped vanadate bounce lasers having high Nd doping.

Key words: Diode-pumped lasers, Thermal lensing, Interferometry

PACS: 42.55.Xi, 65.40.-b

1 Introduction

Diode-pumped solid-state lasers that have high output powers and emit at 1.3- μm have been attracting considerable attention, because of their potential use in a variety of applications, such as laser displays and medical diagnostic systems [1].

A promising method for achieving high-power, high-quality 1.3- μm output involves using a diode-side-pumped bounce-amplifier configuration [2]. This configuration is capable of producing large inversion populations near the pump face when used in conjunction with high Nd doping ($> 1\%$) as a result of strong diode absorption. Minassian *et al.* have successfully demonstrated 13.7-W output from a diode-pumped bounce amplifier based on a Nd:YVO₄ slab, which has a larger stimulated emission cross section than Nd:YAG [3].

In the case of Nd-doped vanadate lasers having 1.3- μm output, a large quantum defect as well as strong excited-state absorption (ESA) induce significant energy dissipation through heat generation in the crystal [4, 5]. Concentration quenching includes multi-phonon decay of the upper laser level and Auger recombination (a nonlinear process in which the energy of one excited Nd ion is transferred to another excited ion, and then dissipated), and it is considered to be important in the thermal loading of slab amplifiers having high Nd doping. Further power scaling of 1.3- μm bounce lasers requires careful thermal management to overcome problems associated with severe heat generation in amplifiers.

Recently, Amarande *et al.* measured thermal-lens effects in bounce amplifiers under non-lasing conditions by using a beam-propagation technique [6]. However, they did not directly measure thermal-lens effects under lasing conditions, neither did they address thermal issues for 1.3- μm laser action.

In this paper, we describe quantitative measurements of thermal-lens effects in a side-pumped Nd:YVO₄ bounce amplifier for 1.3- μm laser operation for the first time.

2 Experiments

2.1 Laser system

A schematic diagram of the used laser cavity is shown in Fig. 1. The amplifier was a 1-at.% Nd-doped *a*-cut YVO₄ slab having dimensions of 2 mm \times 5 mm \times 20 mm. The two end faces (2 mm \times 5 mm facets) of the slab were AR-coated for 1.3- μm , and the pump face (2 mm \times 20 mm facet) was AR-coated for the diode wavelength (808 nm).

The pump diode used was a 55-W CW diode bar array, and its output was focused onto the pump face by a 12.7-mm-focal-length cylindrical lens to be a line having dimensions of ~ 0.2 mm \times 18 mm. The cavity was formed by a high-reflection flat mirror, EM, and an 85 % reflective flat output coupler, OC, for 1342 nm. In order to compensate for the strong thermal lens along the *z*-axis

of the amplifier (vertical thermal lens) and to achieve a good spatial overlap between the ellipsoidal pumped region and the cavity mode, two cylindrical lenses ($f = 50$ mm), VCL, were placed inside the cavity. The distances between the slab and the cylindrical lenses were ~ 50 mm. Initially, the cavity was symmetric with respect to the position of the Nd:YVO₄ amplifier. The total cavity length was ~ 160 mm ($L_1 \sim L_2 \sim 80$ mm). The internal bounce angle with respect to the pump surface of the amplifier was $\sim 10^\circ$.

Figure 2 shows the experimental output power as a function of the pump power. A slope efficiency of 26 % and a lasing threshold of 10 W were measured. The maximum output power was 11.2 W. In order to investigate the cavity stability, the cavity length was extended to ~ 320 mm ($L_1 \sim 80$ mm and $L_2 \sim 240$ mm) making the cavity asymmetric. According to the stability formula for an active resonator [7], this configuration makes the cavity unstable when the thermal-lens power is stronger than $1/L_2$. The cavity became unstable at a pump power of 35-40 W, and a kink in the power curve was observed (see Fig. 2). The thermal lens along the y-axis of the amplifier (horizontal thermal lens) is mainly contributed to the cavity stability, and its power around a pump power of 35 W was estimated to be $\sim 4.2 \text{ m}^{-1}$ ($f = 240$ mm).

2.2 Thermal lens measurement

The experimental setup for thermal-lens measurements in the amplifier is shown in Fig. 3. We employed a holographic lateral-shear interferometric technique [8, 9] to measure the horizontal thermal lens. A green laser having 532-nm output was used as a probe laser. The collimated probe beam passed through the amplifier and the thermal lens distorted its wavefront. After passing through the imaging optics, the distorted probe beam was delivered to a holographic shear plate. The shear plate, including two gratings with different spatial frequencies, enabled the distorted probe beam to interfere with its copy sheared laterally in the xy plane, forming the series of fringes depicted in Fig. 4. The 1st-order diffraction angle was $\sim 30^\circ$. The lateral shear was estimated to be 0.13 mm onto the CCD camera. The imaging optics then imaged the end face of the amplifier onto a CCD camera (COHU-4812).

The spatial phase distortion along the y -axis was retrieved using a Fourier-analysis method initially proposed by Takeda *et al.* [10]. Figure 5 shows the retrieved phase distribution under lasing condition at the pump power of 35-W. The thermal-lens power, D , was determined by fitting the retrieved wavefront with a parabolic function. The measured values were then calibrated for 1342 nm using Sellmeier's equation for Nd:YVO₄ [11]. With this technique, the accuracy of the

measured values was found to be within $\pm 12\%$, as stated in our previous paper [8]. The cavity was asymmetric, and the total length was ~ 320 mm ($L_1 \sim 80$ mm and $L_2 \sim 240$ mm). This configuration can significantly expand the laser mode in the amplifier when the thermal lens becomes strong and the cavity becomes unstable. In order to be able to carefully manage the thermal lens that the laser mode experiences, we also estimated the effective mode sizes in the amplifier from the measured near- and far-fields of the 1.3- μm output. The output coupler could be removed to inhibit laser action.

Experimental plots of the thermal-lens power at various pump powers are shown in Fig. 6. Without laser operation, the thermal-lens power was proportional to the pump power with a slope of $0.11 \text{ m}^{-1}/\text{W}$. The contribution of Auger recombination, observed frequently in highly Nd doped vanadates, was not found to be significant. This might be consistent with the saturation effects of the population in the upper laser level due to strong pumping.

The initial slope of the experimental thermal lens data taken with laser action was $0.14 \text{ m}^{-1}/\text{W}$. The ratio of the two slopes was estimated to be 1.3.

At a pump power of approximately 35 W, a kink in the thermal lens curve appeared. This phenomenon was induced by cavity instability, which reduced the energy dissipation due to ESA. In this case, the measured thermal lens power was 4.4-5.6 m^{-1} . This value is consistent with that estimated from the cavity stability.

4 Discussion

According to the heat-loading formula for end-pumped 1.3- μm lasers based on vanadates having low Nd doping (0.3 at.%), proposed previously by our group, the ratio of the fractional heat loading slopes with and without laser action, R , is given by

$$R = \frac{\eta_{a \sin g}}{\eta_{non}} = \frac{1 - \eta_q \left(\frac{\lambda_p}{\lambda_l} \right) \left(\frac{\sigma_e}{\sigma_e + \sigma_{ESA}} \right)}{1 - \eta_q (1 - \beta) \left(\frac{\lambda_p}{\lambda_f} \right)}, \quad (1)$$

where η_q is the pump quantum efficiency, λ_p and λ_l are the pump and laser wavelengths, respectively, σ_e is the stimulated emission cross section, σ_{ESA} is the ESA cross section, β is the fraction of energy in the upper laser level that decays non-radiatively [12] and λ_f is the mean fluorescence wavelength. For 1.0 at.% Nd-doped vanadates, the value of R must be 1.3.

This value is in good agreement with the experimentally obtained ratio for the thermal-lens

slopes under lasing and non-lasing conditions. Our formula can be extended to account for thermal issues in a 1.3- μm side-pumped bounce vanadate amplifier.

To confirm the value of the experimental fractional heat-loading parameter, η_{lasing} , we also numerically simulated the thermal lens occurring in the amplifier. The thermally induced phase shift distribution in the amplifier was simulated (see Fig. 8) by assuming that heat was removed from the top and bottom faces of the slab so as to maintain them at a constant temperature, and that there was negligible heat flow from the other faces of the slab (see Fig. 7) [13]. We used the experimental parameters given in Table 1.

The spatial distribution of the optical path length, which the laser mode experiences in the bounce amplifier, can be obtained by integrating the phase shift along the optical paths (shown by the red solid line in Fig. 7 in the horizontal direction). By fitting the spatial distribution of the optical path-length change with a parabolic function, the thermal lens power was estimated to be 4.9 m^{-1} at a pump power of 35 W. The mode size in the amplifier was assumed to be 2.3 mm. The simulated thermal lens power is in good agreement with the experimental one.

After replacing the cavity mirrors with the symmetric cavity configuration, we also investigated thermal-lens effects in the amplifier with 1.06- μm laser action. The slope of the thermal lens was measured to be $0.076 \text{ m}^{-1}/\text{W}$. The ratio of the slopes under lasing and non-lasing conditions was 0.69, this value is also consistent with that ($R = 0.71$) theoretically expected by formula (1) [as shown in Fig. 9](#). Our heat-loading formula (1) can also be applied for estimating heat loading in the side-pumped slab amplifier with 1.06- μm laser action.

5 Conclusion

We quantitatively investigated the thermal-lens effects in a side-pumped 1.3- μm Nd:YVO₄ slab bounce amplifier. The thermal lens power during 1.3- μm laser action was 1.3-times larger than that without laser action. We also investigated the 1.3- μm cavity stability by using an asymmetric extended cavity, and found good consistency between the results of both experiments.

The heat-loading formula for end-pumped 1.3- μm lasers based on vanadates having low Nd doping can be extended to account for heat generation in diode-side-pumped Nd-doped vanadate bounce lasers.

Acknowledgement

The authors acknowledge support from the Research Grant (PRESTO) of the Japan Society for the Promotion of Science.

References

- [1] J. Liao, J.-L. He, H. Liu, H.-T. Wang, S. N. Zhu, Y. Y. Zhu, N. B. Ming, *Appl. Phys. Lett.* 82 (2003) 3159-3161
- [2] J. E. Bernard, A. J. Alcock, *Opt. Lett.* 18 (1993) 968-970.
- [3] A. Minassian, M. J. Damzen, *Opt. Commun.* 230 (2004) 191-195.
- [4] L. Fornasiero, S. Kuck, T. Jensen, G. Huber, B. H. T. Chai, *Appl. Phys B.* 67 (1998) 549-553
- [5] M. Okida, M. Itoh, T. Yatagai, H. Ogilvy, J. Piper, T. Omatsu, *Optics Express* 13 (2005) 4909-4915.
- [6] S. A. Amarande, M. J. Damzen, *Opt. Commun.* 265 (2006) 306-313.
- [7] W. Koechner, *Solid-State Laser Engineering*, 5th Ed., (Springer-Verlag, Berlin, 1999) p. 210
- [8] J. L. Blows, J. M. Dawes, T. Omatsu, *J. Appl. Phys.* 83 (1998) 2901-2906.
- [9] J. L. Blows, T. Omatsu, J. Dawes, H. Pask, M. Tateda, *IEEE Photon. Tech. Lett.* 10 (1998) 1727-1729
- [10] M. Takeda, H. Ina, S. Kobayashi, *J. Opt. Soc. Am.* 72 (1982) 156.
- [11] http://www.casix.com/product/prod_cry_yvo4.html
- [12] B. Comaskey, B. Moran, G. Albrecht, R. Beach, *IEEE J. Quantum Electron.* 31 (1995) 1261-1264.
- [13] J. C. Bermudez G., V. J. Pinto-Robledo, A. V. Kir'yanov, M. J. Damzen, *Opt. Commun.* 210 (2002) 75-82
- [14] Y. Sato, T. Taira, N. Pavel, V. Lupei, *Appl. Phys. Lett.* 82 (6) (2003) 844-846.
- [15] V. Lupei, *Opt. Materials* 24 (2003) 353-368.

Table 1
Physical parameters of 1 at. % Nd:YVO₄ slab

Pump quantum efficiency	$\eta_q = 1$ [14]
Non radiative branching ratio	$\beta = 0.17$ [5]
Stimulated emission cross section	$\sigma_e = 4.5 \times 10^{-19} \text{ cm}^2$ (1342 nm) [4] $\sigma_e = 12 \times 10^{-19} \text{ cm}^2$ (1064 nm) [4]
ESA cross section	$\sigma_{\text{ESA}} = 0.5 \times 10^{-19} \text{ cm}^2$ (1342 nm) [4] $\sigma_{\text{ESA}} < 0.15 \times 10^{-19} \text{ cm}^2$ (1064 nm) [4]
Mean fluorescence wavelength	$\lambda_f = 1032 \text{ nm}$ [15]
Refractive index temperature coefficient	$dn/dT = 3.0 \times 10^{-6} \text{ K}^{-1}$ [13]
Absorption coefficient	$\alpha \sim 30 \text{ cm}^{-1}$ [13]
Thermal conductivity	$K = 5.10 \text{ W/(mK)}$ [13]

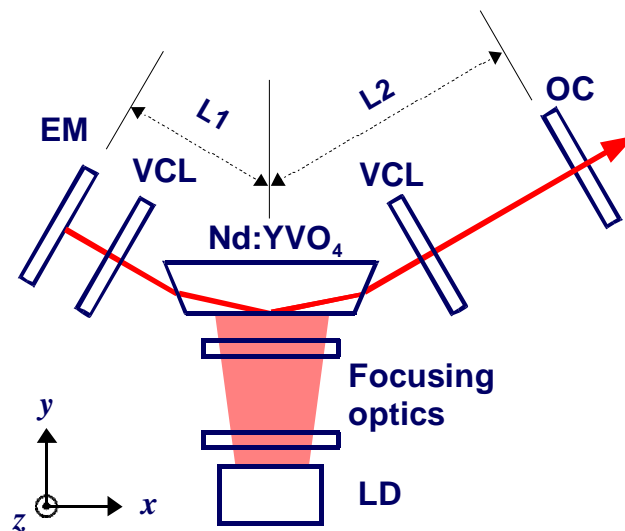


Fig. 1 Experimental setup of laser system. EM is a high-reflection flat mirror. OC is a 85 % reflection output coupler. VCLs are vertical cylindrical lenses.

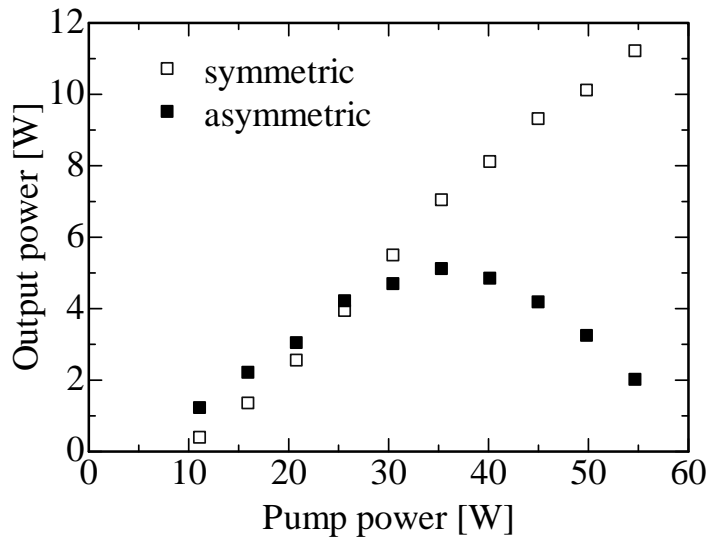


Fig. 2 Output powers for the symmetric and asymmetric cavities

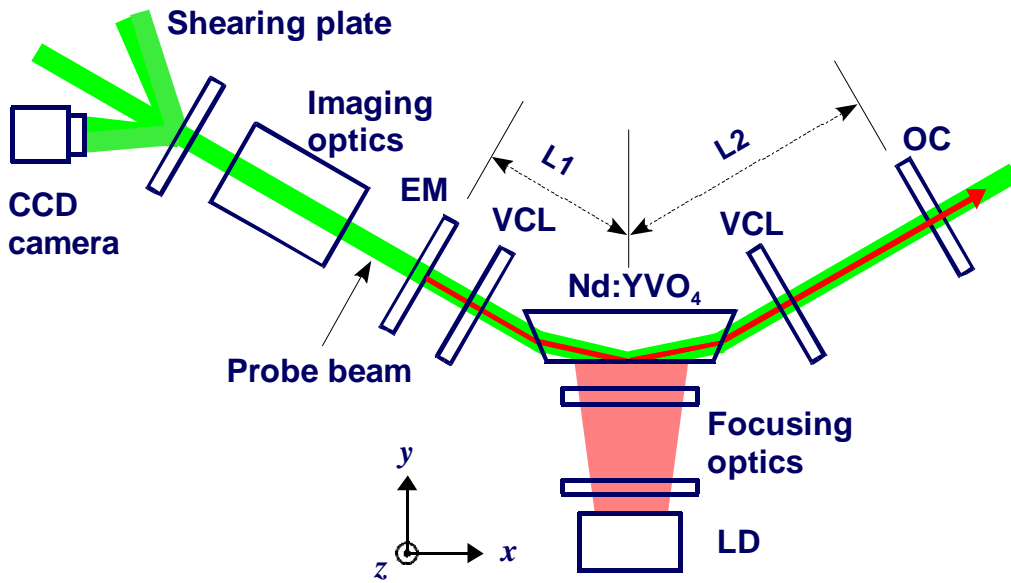


Fig. 3 Experimental setup for wavefront measurement.

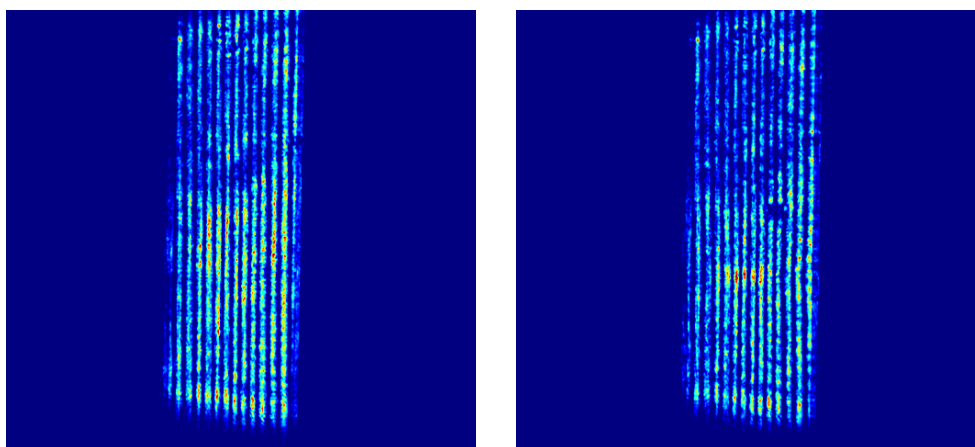


Fig. 4 Interferometric fringe patterns captured on a CCD camera without lasing (left) and with lasing (right) at 35-W pumping

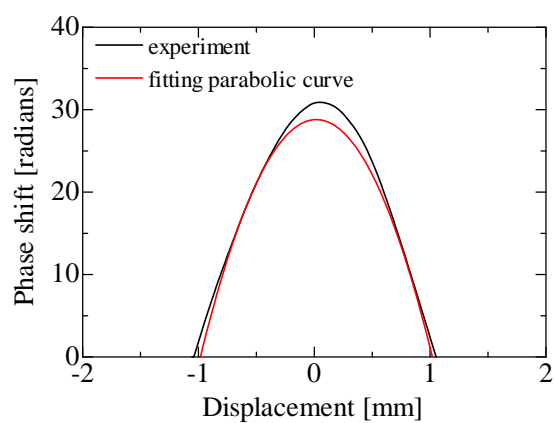


Fig. 5 Retrieved phase distribution and its fitting parabolic curve under lasing condition at the pump power of 35-W.

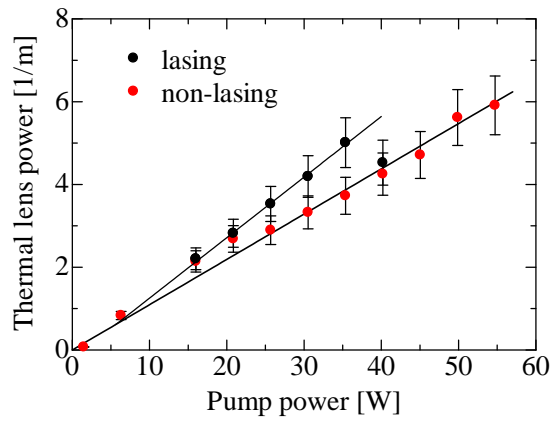


Fig. 6 Horizontal thermal lens power as a function of pump power with and without lasing. The fitted lines with and without laser action coincide at the pump power of 5.6 W (the lasing threshold).

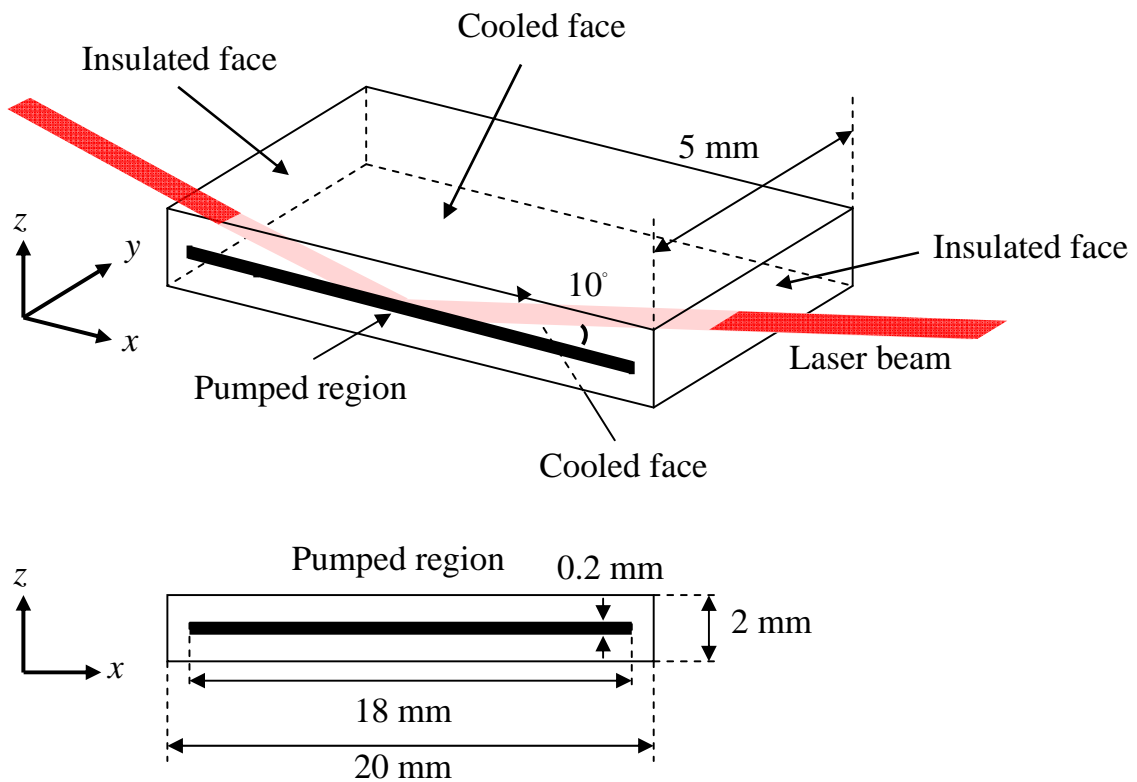


Fig. 7 Model of Nd:YVO₄ slab for numerical simulation.

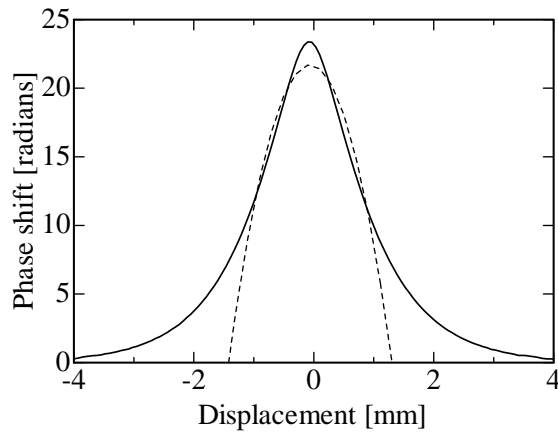


Fig. 8 Numerical simulation results for phase shift profile along y-axis (solid line) for 1342 nm at 35-W pumping (with lasing). The fitting parabolic curve is represented by the dashed line.

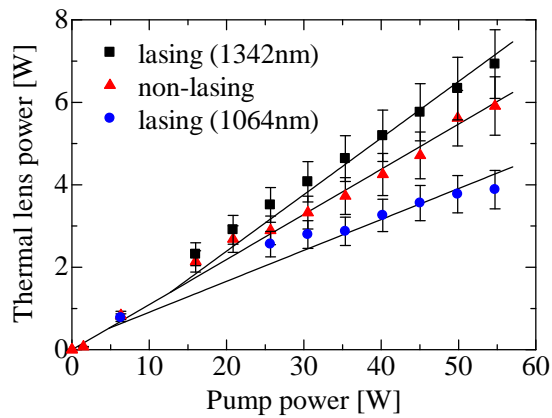


Fig. 9 Thermal lens power as a function of pump power with lasing at 1342 nm, 1064 nm and without lasing in the symmetric cavity. The fitted lines with and without laser action coincide at each lasing thresholds for 1342 nm and 1064 nm. The lasing threshold for 1342 nm and 1064 nm were 12.7 W and 4.9 W respectively.